

Received March 1, 2022, accepted March 14, 2022, date of publication March 22, 2022, date of current version March 30, 2022.

Digital Object Identifier 10.1109/ACCESS.2022.3161549

# A New Calculation Method of the Sensitivity Coefficient for the ERT System

XUAN LI<sup>1</sup>, DA WANG<sup>2</sup>, SHIHONG YUE<sup>2</sup>, DING CHEN<sup>3</sup>, FENG LI<sup>4</sup>,  
AND HUAXIANG WANG<sup>2</sup>, (Senior Member, IEEE)

<sup>1</sup>School of Data Engineering, Tianjin University of Finance and Economics Pearl River College, Tianjin 301811, China

<sup>2</sup>School of Electrical Information and Automation, Tianjin University, Tianjin 300072, China

<sup>3</sup>CCCC Tianjin Dredging Company Ltd., Tianjin 300461, China

<sup>4</sup>CNPC Bohai Directional Drilling Technical Service Company BHDC, Tianjin 300280, China

Corresponding author: Da Wang (da.wang@tju.edu.cn)

This work was supported in part by the National Natural Science Foundation of China under Grant 61973232, and in part by the Pre-Research Major Projects of Tianjin University of Finance and Economics Pearl River College under Grant ZJZD21-10.

**ABSTRACT** Electrical Resistance Tomography (ERT) is a promising technique owing to its low cost, high speed, and visualization features. The sensitivity coefficient plays a significant role in ERT image reconstruction as a priori information. However, the existing methods for calculating sensitivity matrix suffer from poor interpretability and operability. The result leads to an obstacle to improving the quality of the reconstructed images. Therefore, we propose a new sensitivity calculation method that has the advantages of clear physical significance, high robustness, and strong interpretability. We compared the existing and new sensitivity matrices with some metrics, such as correlation coefficient and relative error, and tested the new method's performance by numerical simulations and experiments. The results show that the new sensitivity matrix is feasible and has better performance in ERT imaging reconstruction, especially in the presence of noise.

**INDEX TERMS** Electrical resistance tomography, sensitivity matrix, electromagnetic field theory.

## I. INTRODUCTION

Electrical Resistance Tomography (ERT) is a promising visualization measurement technique with the advantages of high speed, low cost, and strong robustness. The technology aimed to image the conductivity distribution by measuring the boundary response of the excitation signal [1], [2].

The sensitivity matrix is an approximate solution of the Jacobian matrix between measured sensing field and boundary measurement [3], which plays a significant role in ERT image reconstruction as a priori information [4]. However, the sensitivity matrix is poorly conditioned and highly non-linear [5], and the existing sensitivity calculation method is subject to the two problems in their applications.

The first one is that the method is highly dependent on the initial conductivity distribution in the sensing field. When the conductivity has changed significantly, the reconstructed images tend to be low resolution and severe distortion [6].

The associate editor coordinating the review of this manuscript and approving it for publication was Hiram Ponce.

The second one is that the method is poorly interpretable. It uses the finite element analysis method to calculate the sensitivity coefficient. Then, the solution principle is to select the finite elements in the field and use the finite difference equation to replace the partial differential equation to obtain the value of the field function at discrete points [7]. Therefore, the method cannot clearly express the relationship between the sensitivity coefficient and the sensing field.

Based on the above problems, this paper proposes a new sensitivity coefficient calculation method, which defines the sensitivity by using the electromagnetic relationship of the sensing field unit with the electrodes, and the solution is independent of the initial conductivity distribution.

## II. ERT FUNDAMENTALS

This section includes two parts: the principle of ERT and the illustration of sensitivity coefficient.

### A. THE PRINCIPLE OF ERT

In ERT, the problem of solving the potential distribution through the conductivity distribution is the forward

problem [8], which can be expressed as

$$U = F(\sigma) \tag{1}$$

where  $U$  represents the potential distribution,  $\sigma$  denotes the known conductivity distribution, and  $F$  is the forward operator.

The inverse problem of the ERT is to find the distribution of the conductivity  $\sigma$  in the sensitive field based on the measured voltages, which can be written as

$$\sigma = F^{-1}(U) \tag{2}$$

Basically, the relationship between the spatial and electric potential distribution of the conductivity can be derived from Maxwell's equation [9], shown as

$$\nabla \cdot (\sigma \nabla \phi) = 0 \tag{3}$$

where  $\sigma$  and  $\phi$  stand for the investigated domains' electrical conductivity and electrical potential, respectively.

It is possible to collect the information of the spatial distributions by a group of measured boundary voltages. Based on the finite element method (FEM)[10], the linearized and discrete form of (3) can be expressed as

$$\begin{aligned} \Delta \mathbf{U}_{M \times 1} &= \mathbf{S}_{M \times N} \cdot \Delta \boldsymbol{\sigma}_{N \times 1} \\ \text{or } \mathbf{U} &= \mathbf{S} \boldsymbol{\sigma} \end{aligned} \tag{4}$$

where  $\Delta \boldsymbol{\sigma}_{N \times 1}$  is the normalized conductivity vector, and  $\mathbf{S}_{M \times N}$  is a Jacobian matrix, i.e. the sensitivity matrix, giving the sensitivity map from boundary excitations to measurements.  $M$  and  $N$  are the number of boundary measurements and the detected field's inner units (pixels), respectively.

Consequently, the aim of ERT is to find the unknown  $\boldsymbol{\sigma}$  from the known  $\mathbf{U}$  and  $\mathbf{S}$  by solving (4), which can be expressed by the generalized inverse  $\mathbf{S}^{-1}$  as

$$\boldsymbol{\sigma} = \mathbf{S}^{-1} \mathbf{U} \tag{5}$$

The linear back projection (LBP) algorithm is a simple and straightforward method to solve (5) by directly replacing  $\mathbf{S}^{-1}$  with  $\mathbf{S}^T$  [11], namely

$$\boldsymbol{\sigma} = \mathbf{S}^T \mathbf{U} \tag{6}$$

The algorithm is fast and easy to implement but ignores the nonlinearity and pathological nature of the problem, so it is difficult to obtain an exact solution [12]. Therefore, we usually transform solving (6) into solving the optimization problem corresponding to the least-squares error of the equation. That is

$$\|\mathbf{U} - \mathbf{S} \boldsymbol{\sigma}\| \rightarrow \min \tag{7}$$

The algorithms for solving (7) are classified into iterative and non-iterative algorithms. Among the non-iterative algorithms, the Tikhonov regularization (TR) algorithm [13] is the most typical one. It transforms (7) into (8) by adding the regularity term  $G(\boldsymbol{\sigma})$ ,

$$\min f(x) = \|\mathbf{U} - \mathbf{S} \boldsymbol{\sigma}\|_2^2 + \lambda G(\boldsymbol{\sigma}) \tag{8}$$

where  $\lambda$  is a regularization parameter, which is a constant greater than zero. If no other prior information is available, we usually take  $G(\boldsymbol{\sigma})$  to be  $\|\boldsymbol{\sigma}\|_2$ . The optimal analytical solution of (8) is

$$\boldsymbol{\sigma} = (\mathbf{S}^T \mathbf{S} + \lambda \mathbf{I})^{-1} \mathbf{S}^T \mathbf{U} \tag{9}$$

### B. THE ILLUSTRATION OF SENSITIVITY COEFFICIENT

The sensitivity coefficient represents the change rate of electrode potential corresponding to the unit conductivity [14]. The conductivity change in any unit brings a difference in the potential measured at the boundary in the ERT field. As shown in Fig.1(a), the initial distribution of conductivity is uniform, the input current of the  $m$ th electrode pair is  $I$ , the measurement voltage of the  $n$ th electrode pair is  $V$ , and the conductivity of the  $J$ th unit is  $\sigma_J$ .

The excitation and measurement electrodes in Fig.1(b) are the same as in Fig.1(a). When the conductivity increment of the  $J$ th unit is  $\Delta \sigma$  and other units remain unchanged, the voltage increment of the  $n$ th electrode pair will be  $\Delta V$ . The sensitivity of the  $J$ th unit under this excitation state is defined as

$$J = \Delta V / \Delta \sigma \tag{10}$$

To simplify the calculation process, two assumptions were given [16]. The one is that the higher-order nonlinear terms in the calculation have less impact on the results. The other is that there are no infinite values near the electrodes. In this way, the nonlinear problem in the sensitivity solution process is approximately reduced to a linear problem. Hence, according to the Geselowitz theory [15], the sensitivity for the ERT system can be defined as

$$J_{ij} = - \int \frac{\nabla \phi_i}{I_i} \cdot \frac{\nabla \phi_j}{I_j} dx dy \tag{11}$$

where  $J_{ij}$  is the sensitivity coefficient of the  $j$ th electrode pair to the  $i$ th electrode pair;  $\phi_i$  and  $\phi_j$  are the potential distribution of the  $i$ th electrode and  $j$ th electrode when the excitation currents are the  $I_i$  and  $I_j$ , respectively.

Due to the simplified treatment of the calculation process, this sensitivity coefficient calculation method has some limitations in the applications.

We use a typical 16-electrode ERT system to explain the ERT measuring principle [17]. Fig.1(c) shows the ERT measuring process in  $\Omega$ . Firstly, the excitation current  $I$  is injected into the first and second electrodes, and 13 measurements are obtained between the other electrodes. Then,  $I$  is injected into the second and third electrodes. Again 13 measured values are obtained. This process is repeated until all 16 electrodes are excited. Thus, 208 measurements are obtained to calculate the parameters in  $\Omega$ .

Cutting the circumscribed square of the circular field into 32 equal parts on each side, then 812 units will fall in the circle. Therefore, the sensitivity matrix can be defined by the  $208 \times 812$  sensitivity coefficients for the 16-electrode ERT system.

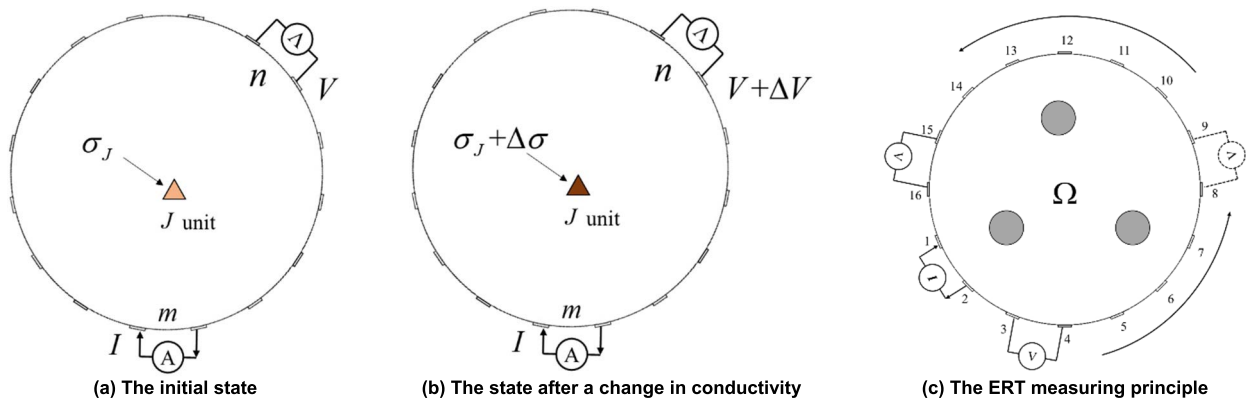


FIGURE 1. The ERT principle diagrams.

### III. A NEW SENSITIVITY CALCULATION METHOD

#### A. THE ELECTRIC FIELD GENERATED BY A LONG STRAIGHT CONDUCTOR

For a long, straight, and thin conductor in a vacuum, the potential can be derived as follows [18]

$$\varphi = \frac{\tau}{2\pi\epsilon_0} \ln \frac{r_M}{r} \quad (12)$$

where  $\tau$  is the charge density,  $\epsilon_0$  is the relative permittivity,  $r_M$  is the distance between the potential reference point and the conductor, and  $r$  is the distance between the field point and the conductor.

It is known that the electric field  $\mathbf{E}$  generated by a set of stationary charges can be written as the gradient of a scalar potential

$$\mathbf{E} = -\nabla\varphi \quad (13)$$

Hence, the electric field of the long thin conductor can be written as

$$\mathbf{E} = \frac{\tau}{2\pi\epsilon_0 r} \mathbf{e}_r \quad (14)$$

where  $\mathbf{e}_r$  is the unit vector in the same direction with  $\mathbf{r}$ .

As shown in Fig. 2(a), the 1st and 2nd electrodes represent the excitation electrodes, and the 7th and 8th electrodes represent the measurement electrodes. Therefore, the electric field  $\mathbf{E}_M$  at any point  $M$  is

$$\begin{aligned} \mathbf{E}_M &= \frac{\tau}{2\pi\epsilon_0} \left( \frac{\mathbf{e}_{r_{1M}}}{r_{1M}} + \frac{\mathbf{e}_{r_{M2}}}{r_{M2}} \right) \\ &= \frac{\tau}{2\pi\epsilon_0} \left( \frac{\mathbf{r}_{1M}}{|\mathbf{r}_{1M}|^2} + \frac{\mathbf{r}_{M2}}{|\mathbf{r}_{M2}|^2} \right) \end{aligned} \quad (15)$$

where vector  $\mathbf{r}_{1M}$  points to the point  $M$  from the 1st electrode and vector  $\mathbf{r}_{M2}$  points to 2nd electrode from the point  $M$ .

Set

$$\mathbf{a} = \frac{\mathbf{r}_{1M}}{|\mathbf{r}_{1M}|^2} + \frac{\mathbf{r}_{M2}}{|\mathbf{r}_{M2}|^2} \quad (16)$$

The module value of  $\mathbf{E}_M$  can be written as

$$|\mathbf{E}_M| = \frac{\tau}{2\pi\epsilon_0} |\mathbf{a}| \quad (17)$$

#### B. THE ELECTRIC FIELD GENERATED BY ELECTRIC DIPOLES

As shown in Fig.2(b), there is a pair of dipoles with the distance of  $d$  carrying equal charges  $q$  and opposite signs. Point  $O$  is the midpoint of the dipoles, and Point  $P$  is a point in space. According to Coulomb's law [19], the potential generated by the dipoles at the point  $P$  is

$$\varphi_P = \frac{q}{4\pi\epsilon_0} \left( \frac{1}{r_+} - \frac{1}{r_-} \right) \quad (18)$$

where  $r_+$  is the distance between point  $P$  and the positive charge, and  $r_-$  is the distance between point  $P$  and the negative charge.

Suppose the distance between the point  $P$  and the point  $O$  is  $r$ , when  $r \gg d$ , we have

$$\varphi_P = \frac{qd \cos \theta}{4\pi\epsilon_0 r^2} \quad (19)$$

where  $\theta$  is the angle between  $d$  and  $r$ .

And the electric field  $\mathbf{E}_q$  generated by a point charge  $q$  is

$$\mathbf{E}_q = \frac{q}{4\pi\epsilon_0 r^2} \mathbf{e}_r \quad (20)$$

Hence, the electric field generated by the dipoles at point  $O$  is

$$\begin{aligned} |\mathbf{E}_O| &= |\mathbf{E}_{+q}| + |\mathbf{E}_{-q}| \\ &= \frac{q}{4\pi\epsilon_0 (\frac{d}{2})^2} + \frac{q}{4\pi\epsilon_0 (\frac{d}{2})^2} \\ &= \frac{2q}{\pi\epsilon_0 d^2} \end{aligned} \quad (21)$$

#### C. THE NEW CALCULATION METHOD OF THE SENSITIVITY COEFFICIENT

In the ERT system, a current field excited by a stable current is stable, and it can be equivalent to the electric field generated by a pair of dipoles.

As shown in Fig.2(c), the electric field generated by the 1st electrode and 2nd electrode at point  $M$  can be equivalent to the electric field generated by the dipoles centered by point

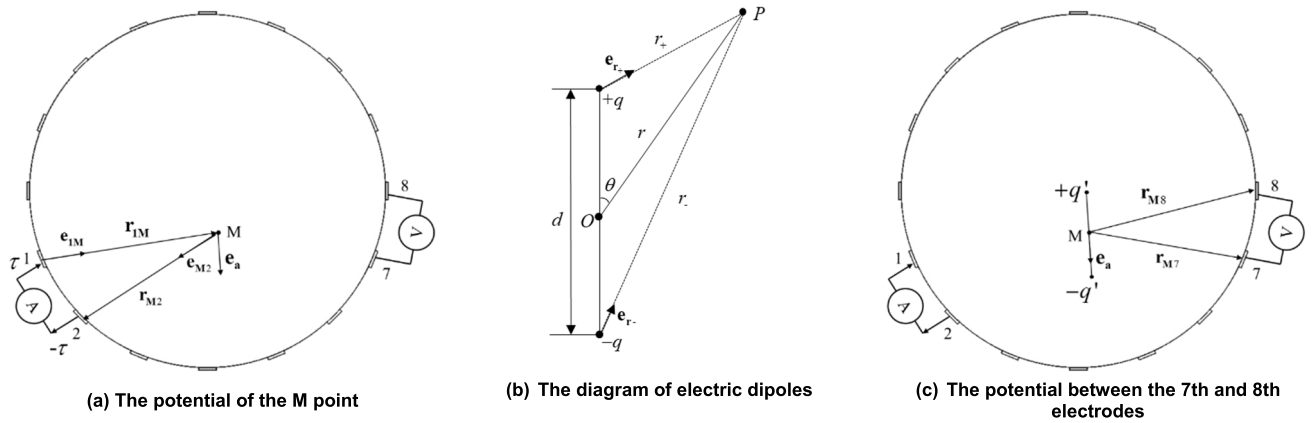


FIGURE 2. The electric potential calculation diagrams.

Owith the charge of  $q'$  and the distance of  $d_0$ . According to (17) and (21), it is

$$q' = \frac{\tau}{4} d_0^2 |\mathbf{a}| \quad (22)$$

Therefore, combined with (19), the potentials generated by the dipoles at the 7th and 8th electrodes are

$$\left\{ \begin{aligned} \varphi_7 &= \frac{q' d_0 \cos \alpha}{4\pi \epsilon_0 |\mathbf{r}_{M7}|^2} \\ &= \frac{\tau d_0^3}{16\pi \epsilon_0} \frac{|\mathbf{a}|}{|\mathbf{r}_{M7}|^2} \cos \alpha \\ \varphi_8 &= \frac{q' d_0 \cos \beta}{4\pi \epsilon_0 |\mathbf{r}_{M8}|^2} \\ &= \frac{\tau d_0^3}{16\pi \epsilon_0} \frac{|\mathbf{a}|}{|\mathbf{r}_{M8}|^2} \cos \beta \\ \cos \alpha &= \frac{\mathbf{a} \cdot \mathbf{r}_{M7}}{|\mathbf{a}| |\mathbf{r}_{M7}|} \\ \cos \beta &= \frac{\mathbf{a} \cdot \mathbf{r}_{M8}}{|\mathbf{a}| |\mathbf{r}_{M8}|} \end{aligned} \right. \quad (23)$$

Since  $\tau$  and  $d_0$  are fixed, the potentials can be written as

$$\left\{ \begin{aligned} \varphi_7 &= c \frac{\mathbf{a} \cdot \mathbf{r}_{M7}}{|\mathbf{r}_{M7}|^3} \\ \varphi_8 &= c \frac{\mathbf{a} \cdot \mathbf{r}_{M8}}{|\mathbf{r}_{M8}|^3} \end{aligned} \right. \quad (24)$$

where

$$c = \tau d_0^3 / 16\pi \epsilon_0 \quad (25)$$

Then the sensitivity of the  $m$ th unit excited by the 1st and 2nd electrodes and measured by the 7th and

8th electrodes is

$$\begin{aligned} S_{M7,8} &= \varphi_7 - \varphi_8 \\ &= c \left( \frac{\mathbf{a} \cdot \mathbf{r}_{M7}}{|\mathbf{r}_{M7}|^3} - \frac{\mathbf{a} \cdot \mathbf{r}_{M8}}{|\mathbf{r}_{M8}|^3} \right) \end{aligned} \quad (26)$$

Therefore, the sensitivity coefficients of 812 units can be calculated in the same way. For a 16-electrode ERT system with adjacent excitation and adjacent measurements, we will get the sensitivity matrix with  $208 \times 812$  dimensions.

In summary, the new sensitivity calculation method is independent of the conductivity in the sensing field, which implies that it has better robustness.

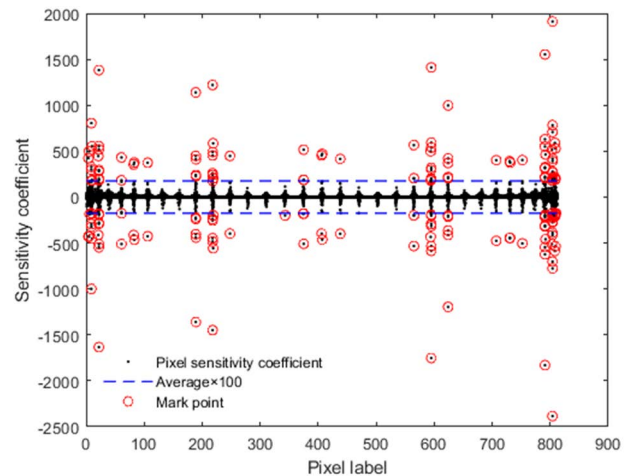
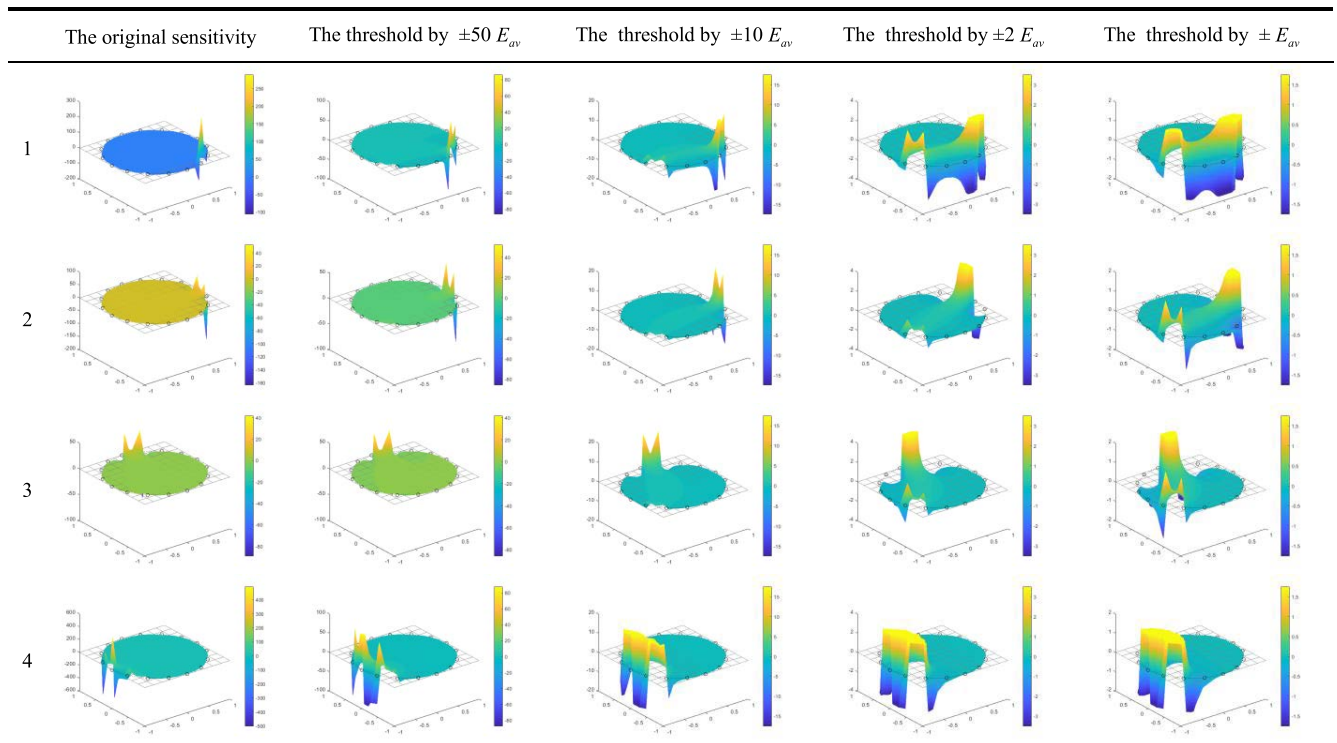


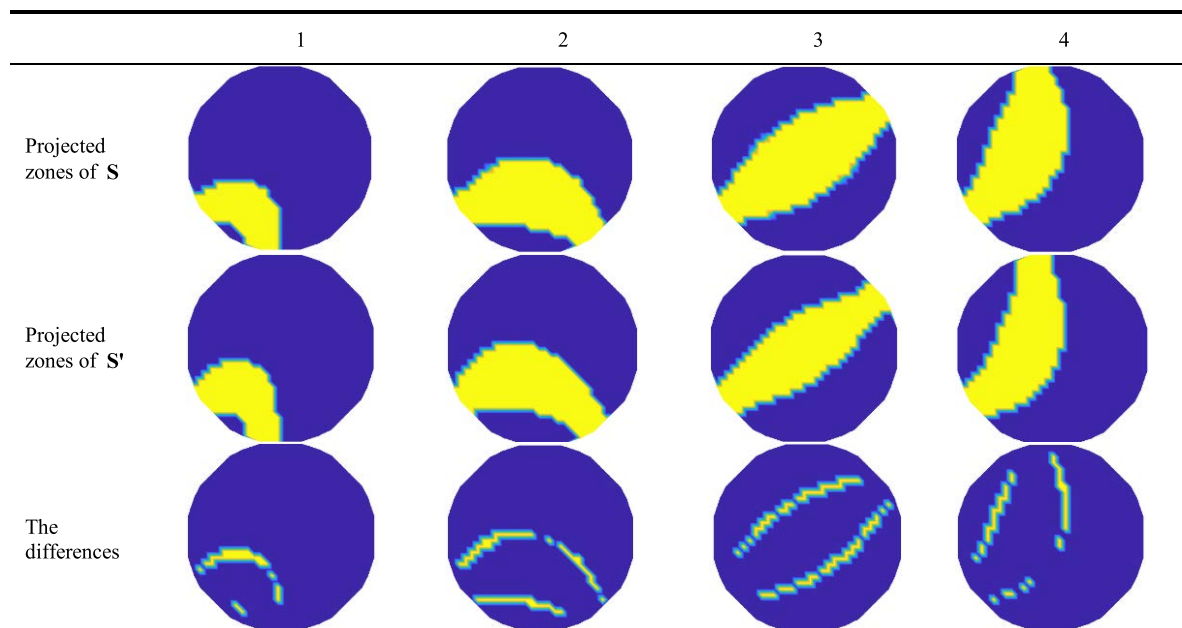
FIGURE 3. The scatter plot of the sensitivity matrix.

Fig.3 is the scatter plot of the sensitivity matrix. Let  $E_{av}$  be the average absolute value of the sensitivity, and the blue dotted lines represent the value of plus or minus one hundred times of  $E_{av}$ . The points marked by red circles are all outside the blue line. The scatter plot shows that the new calculation method will result in infinite values in the vicinity of the electrodes. These values seriously affect the image reconstruction quality. In what follows, we will choose the appropriate threshold to truncate the sensitivity coefficient.

**TABLE 1.** The comparison of the sensitivity coefficient under different thresholds.



**TABLE 2.** Comparisons of the projected zones.



**D. THE SELECTION OF THE SENSITIVITY COEFFICIENT THRESHHOLD**

In practice, the conductivity of neighboring units does not change abruptly. Therefore, the infinite values in the vicinity

of the electrodes are introduced by the computational bias. We use the threshold truncation method to correct the sensitivity coefficient. When the modulus of the sensitivity coefficient is greater than the threshold value, we replace it with

TABLE 3. The images reconstructed by the sensitivity matrices.

	Model 1	Model 2	Model 3	Model 4
The original images				
The reconstructed images using S without noises				
The reconstructed images using S' without noises				
The reconstructed images using S with noises				
The reconstructed images using S' with noises				

the threshold. To find the appropriate threshold, we present the sensitivity maps under different thresholds, as shown in Table 1.

Due to infinite values, the original sensitivity map is flat and shows no saddle shape. As we keep decreasing the truncation threshold, the sensitivity map becomes more and more saddle-like. In addition, the positive and negative projection regions are gradually distinguished. Finally, we set the truncation threshold to plus or minus  $E_{av}$ , and the sensitivity map is well saddle-shaped, which is more favorable for image reconstruction.

IV. THE COMPARISON OF SENSITIVITY COEFFICIENTS

In this section, we mainly compare the new sensitivity matrix with the existing one to verify the validity. We simulate the image reconstruction process in the platform of COMSOL and MATLAB on a PC with the Intel I5-6500 CPU and 8 GB memory. The excitation measurement mode is adjacent excitation and adjacent measurement.

A. DIFFERENCE BETWEEN THE EXISTING AND NEW SENSITIVITY COEFFICIENTS

We normalize the existing and new sensitivity coefficient to the interval [0,1] and calculate the average difference using (27).

$$\Delta s = |S - S'| / 812 \tag{27}$$

where  $S$  and  $S'$  denote the existing and new sensitivity matrix, respectively. The calculation results show that the average difference between them is less than 8%, and the similarity is high. Therefore, combined with the sensitivity maps, we conclude that the new sensitivity coefficient is consistent with the existing one.

B. COMPARISONS OF THE PROJECTED ZONES

Any measurement is generated by the combined effect of positive and negative projection areas. We can evaluate these two sensitivity coefficients by comparing the projection areas. As shown in Table 2, the blue area represents the negative

sensitivity area, and the yellow one means the opposite. By calculation, these projected zones have 25, 46, 59, and 39 different pixels, respectively. The difference is less than 10% compared to the whole pixels in the field. The results imply that the new sensitivity coefficient has similar projection areas to the existing one.

### C. THE COMPARISON OF THE CALCULATION TIME

In the simulation, the time consumed by the new sensitivity matrix is about 0.3 seconds, while the existing matrix is about 11 seconds. Therefore, the new sensitivity matrix has an advantage in computation time.

As has been said, the new sensitivity matrix is consistent with the existing one, and they have similar projection areas and sensitivity maps. Besides, the new sensitivity matrix is relatively easy to solve and consumes less time. Furthermore, since the calculation method does not rely on the initial conductivity value but only on the position information, it is also suitable for applications where the conductivity varies widely.

## V. IMAGE RECONSTRUCTION

This section evaluates the existing and the new sensitivity matrices by two aspects: 1) numerical simulations; 2) experiments.

### A. NUMERICAL SIMULATIONS

In practice, the LBP algorithm is one of the most widely used image reconstruction algorithms due to its simplicity and imaging speed. The LBP algorithm directly replaces the inverse of the sensitivity matrix by its transpose, which is straightforward. Therefore, LBP is more suitable for evaluating the sensitivity coefficients in image reconstruction [20].

We used the simulated data to reconstruct the images using the existing and new sensitivity matrices, respectively, and the reconstruction algorithm was the LBP algorithm. Then we evaluate the image reconstruction results with correlation coefficients and relative errors.

The correlation coefficient [21] between the original and reconstructed images is defined as

$$CC = \frac{\sum_{i=1}^l (\sigma_i - \bar{\sigma})(\sigma_i^* - \bar{\sigma}^*)}{\{\sum_{i=1}^l (\sigma_i - \bar{\sigma})^2 \sum_{i=1}^l (\sigma_i^* - \bar{\sigma}^*)^2\}^{1/2}} \quad (28)$$

where CC is correlation coefficient,  $\sigma$  is the calculated conductivity, and  $\sigma^*$  is the actual one in simulation distribution.  $\sigma_i$  and  $\sigma_i^*$  are the  $i$ th elements of  $\sigma$  and  $\sigma^*$ , respectively;  $\bar{\sigma}$  and  $\bar{\sigma}^*$  are the mean values of  $\sigma$  and  $\sigma^*$ , respectively;  $l$  denotes the pixel number of  $\sigma$ .

Alternatively, we calculate the relative error between reconstructed and original images as [22]

$$RE = \|\sigma - \sigma^*\|_2 / \|\sigma^*\|_2 \quad (29)$$

where  $RE$  is the relative error.

In simulations, we chose four typical permittivity distributions for numerical simulation with a 16-electrode ERT sensor with 208 measurements. The conductivities of the background and these blocks in the object were set as 1S/m(blue) and 2S/m(yellow), respectively. Table 3 shows all the original and reconstructed images.

First, the images were reconstructed by the simulated data without noises in different sensitivity matrices. Then, we added the Gaussian white noise with a signal-to-noise ratio of 60 dB to the simulated data and reconstructed them again.

By comparing the reconstructed images of Model 1 and Model 3, we can see that the images can be performed correctly under the LBP algorithm using both existing and new sensitivity matrices without noises. However, the images reconstructed by the new sensitivity have clearer boundaries and fewer artifacts.

By comparing the reconstructed images of model 2 and model 4, the images are not good with both existing and new sensitivity matrices, which are affected by the defects of the LBP algorithm itself. Nevertheless, the new sensitivity matrix has better performance than the existing ones.

Furthermore, whether using the new or existing sensitivity matrix, the images reconstructed by the simulated data with noises does not restore the original model well. The image reconstruction quality was affected by increased artifacts and unclear boundaries. However, the new sensitivity matrix still performs better than the existing one. This result shows that the new sensitivity matrix is better in robustness.

TABLE 4. The correlation coefficients.

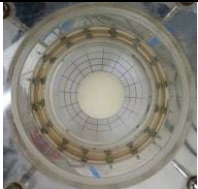
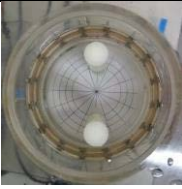
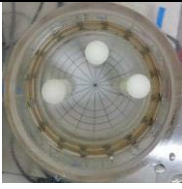
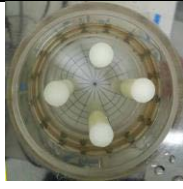
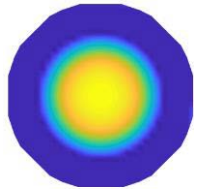
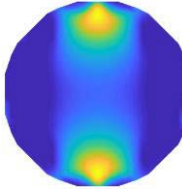
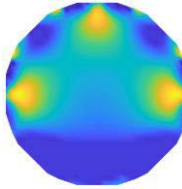
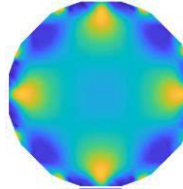
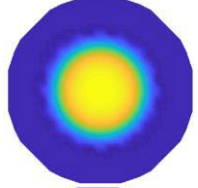
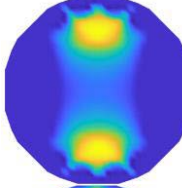
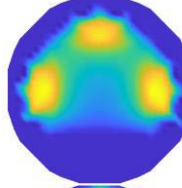
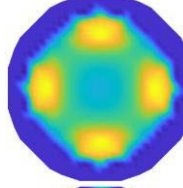
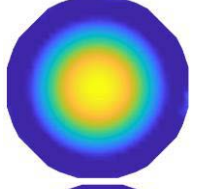
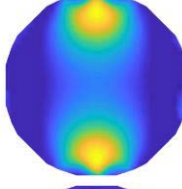
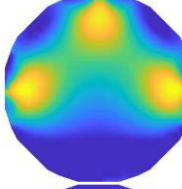
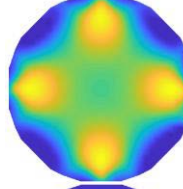
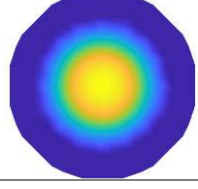
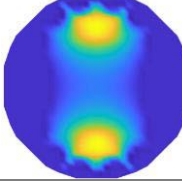
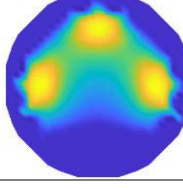
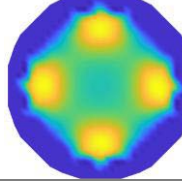
	Model 1	Model 2	Model 3	Model 4
CC using $\mathbf{S}$ without noises	0.36	0.02	0.29	0.24
CC using $\mathbf{S}'$ without noises	0.82	0.11	0.78	0.53
CC using $\mathbf{S}$ with noises	0.28	0.01	0.22	0.17
CC using $\mathbf{S}'$ with noises	0.75	0.08	0.61	0.44

TABLE 5. The relative imaging errors.

	Model 1	Model 2	Model 3	Model 4
RE using $\mathbf{S}$ without noises	1.05	2.13	0.79	0.87
RE using $\mathbf{S}'$ without noises	0.61	1.18	0.58	0.75
RE using $\mathbf{S}$ with noises	1.36	2.23	0.96	1.15
RE using $\mathbf{S}'$ with noises	0.77	1.51	0.72	0.87

The above observations can further be illustrated by the relative errors and the correlation coefficients of the reconstructed images. Table 4 and 5 shows the correlation

**TABLE 6.** The reconstructed images by experiments.

	Experiment 1	Experiment 2	Experiment 3	Experiment 4
the experiment photos				
the images reconstructed by LBP using $S$				
the images reconstructed by LBP using $S'$				
the images reconstructed by TR using $S$				
the images reconstructed by TR using $S'$				

coefficients and relative errors in the four simulation models by the two sensitivity coefficients.

According to the Tables, the reconstructed images using the new sensitivity matrix have higher correlation coefficients and lesser imaging errors, regardless of the effect of noise. The results are consistent with the images.

### B. EXPERIMENTAL RESULTS

The experimental ERT data collection system consists of a sensor with 16 electrodes and a digital hardware system designed by Tianjin University [23], and an adjacent exciting and adjacent measuring mode is applied. The excitation current is a sinusoidal signal, and its amplitude and frequency are 10mA and 100kHz. We used saltwater and nylon rods to simulate different material distributions with the conductivity of 0.1 and almost 0S/m, respectively. In addition, the inner diameter of the measurement field was 160 mm, and the diameter of the nylon rod in the first experiment was 40 mm, except for the others, which were 22 mm. In addition, we chose two

algorithms, LBP and TR, for image reconstruction, and the results are shown in Table 6.

The reconstructed images show that the reconstructed images using the new sensitivity matrix are more accurate and have fewer artifacts than those using the existing one for both the LBP and TR algorithm. This result is consistent with the simulation results.

In sum, according to the above simulated and experimental results, we can make some conclusions as follows:

1) The reconstructed images using the new sensitivity matrix are consistent with the original objects. Therefore, the new calculation method of sensitivity coefficient is feasible.

2) Compared with the existing sensitivity matrix, the reconstructed target using the new sensitivity coefficient matrix has fewer artifacts near the electrodes.

3) The images reconstructed by the new sensitivity matrix are more accurate by contrasting with the correlation coefficients and relative errors.



4) The new sensitivity matrix is more effective with noises than the existing one, indicating that the new sensitivity matrix is better in terms of robustness.

## VI. CONCLUSION

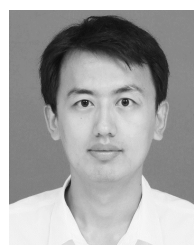
This paper proposes a new sensitivity calculation method, which does not rely on the initial conductivity value but only on the position information. Thus, the new calculation method is more intuitive and physically interpretable. We compared the existing and new sensitivity matrices by simulations and experiments. The results indicate that the new sensitivity matrix has less time consumption and lower noise near the electrodes. Moreover, the images reconstructed by the new sensitivity matrix are more consistent with the actual positions, and the artifacts near the electrode are fewer, especially in terms of noises. According to electrostatic analogy and magnetoelectric analogy, electrical capacitance tomography (ECT) and electromagnetic tomography (EMT) can directly use the new method for image reconstruction [24]. It can be more suitable for various image reconstruction algorithms by optimizing the computation and imaging process. Therefore, the proposed sensitivity calculation method provides a new idea for further improving the spatial resolution of the ERT technology.

## REFERENCES

- [1] Z. Cui, Q. Wang, Q. Xue, W. Fan, L. Zhang, Z. Cao, B. Sun, H. Wang, and W. Yang, "A review on image reconstruction algorithms for electrical capacitance/resistance tomography," *Sensor Rev.*, vol. 36, no. 4, pp. 429–445, Sep. 2016, doi: [10.1108/sr-01-2016-0027](https://doi.org/10.1108/sr-01-2016-0027).
- [2] C. Tan, S. Lv, F. Dong, and M. Takei, "Image reconstruction based on convolutional neural network for electrical resistance tomography," *IEEE Sensors J.*, vol. 19, no. 1, pp. 196–204, Jan. 2019, doi: [10.1109/JSEN.2018.2876411](https://doi.org/10.1109/JSEN.2018.2876411).
- [3] Z. Huang, B. Wang, and H. Li, "Application of electrical capacitance tomography to the void fraction measurement of two-phase flow," *IEEE Trans. Instrum. Meas.*, vol. 52, no. 1, pp. 7–12, Feb. 2003, doi: [10.1109/tim.2003.809087](https://doi.org/10.1109/tim.2003.809087).
- [4] D. T. Nguyen, C. Jin, A. Thiagalingam, and A. L. McEwan, "A review on electrical impedance tomography for pulmonary perfusion imaging," *Physiol. Meas.*, vol. 33, no. 5, pp. 695–706, May 2012, doi: [10.1088/0967-3334/33/5/695](https://doi.org/10.1088/0967-3334/33/5/695).
- [5] M. Mallach, M. Gevers, P. Gebhardt, and T. Musch, "Fast and precise soft-field electromagnetic tomography systems for multiphase flow imaging," *Energies*, vol. 11, no. 5, p. 1199, May 2018, doi: [10.3390/en11051199](https://doi.org/10.3390/en11051199).
- [6] S. Yue, Y. Zhang, Y. Zhao, and H. Wang, "Updating algorithm for sensitivity coefficient of electrical tomography," *J. Tianjin Univ., Sci. Technol.*, vol. 50, no. 12, pp. 1227–1234, 2017.
- [7] M. Ding, S. Yue, J. Li, Y. Wang, and H. Wang, "Second-order sensitivity coefficient based electrical tomography imaging," *Chem. Eng. Sci.*, vol. 199, pp. 40–49, May 2019, doi: [10.1016/j.ces.2019.01.020](https://doi.org/10.1016/j.ces.2019.01.020).
- [8] S. Li, H. Wang, T. Liu, Z. Cui, J. N. Chen, and Z. Xia, "A fast Barzilai-Borwein gradient projection for sparse reconstruction algorithm based on 3D modeling: Application to ERT imaging," *IEEE Access*, vol. 9, pp. 152913–152922, 2021, doi: [10.1109/ACCESS.2021.3127695](https://doi.org/10.1109/ACCESS.2021.3127695).
- [9] Z. Q. Chen and F. J. Paoloni, "An integral equation approach to electrical conductance tomography," *IEEE Trans. Med. Imag.*, vol. 11, no. 4, pp. 570–576, Dec. 1992, doi: [10.1109/42.192693](https://doi.org/10.1109/42.192693).
- [10] M. Wang, "Inverse solutions for electrical impedance tomography based on conjugate gradients methods," *Meas. Sci. Technol.*, vol. 13, no. 1, pp. 101–117, Jan. 2002, doi: [10.1088/0957-0233/13/1/314](https://doi.org/10.1088/0957-0233/13/1/314).
- [11] C. J. Kotre, "A sensitivity coefficient method for the reconstruction of electrical impedance tomograms," *Clin. Phys. Physiol. Meas.*, vol. 10, no. 3, p. 275, 1989, Aug. 1989, doi: [10.1088/0143-0815/10/3/008](https://doi.org/10.1088/0143-0815/10/3/008).
- [12] F. Santosa and M. Vogelius, "A backprojection algorithm for electrical impedance imaging," *SIAM J. Appl. Math.*, vol. 50, no. 1, pp. 216–243, 1990.
- [13] M. Vauhkonen, D. Vadasz, P. A. Karjalainen, E. Somersalo, and J. P. Kaipio, "Tikhonov regularization and prior information in electrical impedance tomography," *IEEE Trans. Med. Imag.*, vol. 17, no. 2, pp. 285–293, Apr. 1998, doi: [10.1109/42.700740](https://doi.org/10.1109/42.700740).
- [14] G. Engl, "The modeling and numerical simulation of gas flow networks," *Numerische Math.*, vol. 72, no. 3, pp. 349–366, Jan. 1996.
- [15] Z. Wang, S. Yue, H. Wang, and Y. Wang, "Data preprocessing methods for electrical impedance tomography: A review," *Physiol. Meas.*, vol. 41, no. 9, Sep. 2020, Art. no. 09TR02, doi: [10.1088/1361-6579/abb142](https://doi.org/10.1088/1361-6579/abb142).
- [16] P. Yan, S. Wang, and L. Shi, "Electrical impedance tomography based on sensitivity theorem with singular value decomposition," in *Proc. IEEE Eng. Med. Biol. 27th Annu. Conf.*, Jan. 2006, pp. 1488–1491.
- [17] A. J. Jaworski and G. Meng, "On-line measurement of separation dynamics in primary gas/oil/water separators: Challenges and technical solutions—A review," *J. Petroleum Sci. Eng.*, vol. 68, nos. 1–2, pp. 47–59, Sep. 2009, doi: [10.1016/j.petrol.2009.06.007](https://doi.org/10.1016/j.petrol.2009.06.007).
- [18] J. R. Wait, "Theory of wave propagation along a thin wire parallel to an interface," *Radio Sci.*, vol. 7, no. 6, pp. 675–679, 1972.
- [19] S. Homma, Y. Nakajima, T. Musha, Y. Okamoto, and B. He, "Dipole-tracing method applied to human brain potentials," *J. Neurosci. Methods*, vol. 21, nos. 2–4, pp. 195–200, Oct. 1987.
- [20] Z. Xu, Y. Jiang, B. Wang, Z. Huang, H. Ji, and H. Li, "Image reconstruction performance of a 12-electrode CCERT sensor under five different excitation patterns," *IEEE Access*, vol. 6, pp. 65783–65795, 2018, doi: [10.1109/ACCESS.2018.2878583](https://doi.org/10.1109/ACCESS.2018.2878583).
- [21] C. G. Xie, S. M. Huang, C. P. Lenn, A. L. Stott, and M. S. Beck, "Experimental evaluation of capacitance tomographic flow imaging systems using physical models," *IEE Proc.-Circuits, Devices Syst.*, vol. 141, no. 5, pp. 357–368, 1994.
- [22] Q. Wang, H. Wang, Z. Cui, Y. Xu, and C. Yang, "Fast reconstruction of electrical resistance tomography (ERT) images based on the projected CG method," *Flow Meas. Instrum.*, vol. 27, pp. 37–46, Oct. 2012, doi: [10.1016/j.flowmeasinst.2012.03.009](https://doi.org/10.1016/j.flowmeasinst.2012.03.009).
- [23] Z. Cui, H. Wang, L. Tang, L. Zhang, X. Chen, and Y. Yan, "A specific data acquisition scheme for electrical tomography," in *Proc. IEEE Instrum. Meas. Technol. Conf.*, May 2008, pp. 726–729.
- [24] B. Sun, S. Yue, Z. Cui, and H. Wang, "A new linear back projection algorithm to electrical tomography based on measuring data decomposition," *Meas. Sci. Technol.*, vol. 26, no. 12, Dec. 2015, Art. no. 125402, doi: [10.1088/0957-0233/26/12/125402](https://doi.org/10.1088/0957-0233/26/12/125402).



**XUAN LI** was born in December 1988. She received the master's degree in mathematics from Tianjin University, in 2014. In 2014, she joined the Tianjin University of Finance and Economics Pearl River College, as a Lecturer. Her research interests include control theory and application, numerical calculation, and electrical engineering and technology.



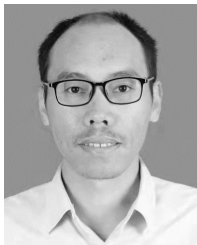
**DA WANG** was born in February 1987. He received the master's degree in control science and engineering from Tianjin University, in 2013. In 2017, he joined the School of Electrical Information and Automation, Tianjin University, as an Engineer. His research interests include electrical tomography, electronic technology, and high-power supply.



**SHIHONG YUE** received the M.S. degree from the Xi'an University of Technology, in 1997, and the Ph.D. degree from Xi'an Jiaotong University, Xi'an, China, in 2000. From 2000 to 2004, he was a Postdoctoral Researcher with the Institute of Industrial Process Control, Zhejiang University, Hangzhou, China. He is currently a Professor with Tianjin University, Tianjin, China. His current research interests include electrical tomography, medical image processing, and data mining.



**FENG LI** was born in August 1987. He received the bachelor's degree in engineering from the Tianjin University of Science and Technology, in 2010. In 2010, he joined CNPC Bohai Drilling-Engineering Company Ltd., as a Directional Drill Engineer, mainly responsible for drilling trajectory control and downhole low-quality data monitoring work, transferred back to the company's marketing and production coordination department, in 2015, engaged in the market operation.



**DING CHEN** received the master's degree in marine engineering from Dalian Maritime University, in 2011. In 2011, he joined CCCC Tianjin Dredging Company Ltd., as an Engineer. His research interests include dredging engineering intelligence and electrification.



**HUAXIANG WANG** (Senior Member, IEEE) received the degree from Tianjin University, Tianjin, China. He is currently a Professor with the School of Electrical and Information Engineering, Tianjin University. His current research interests include sensing techniques and information processing, process parameter detection and control systems, and intelligent instrumentation.

...